CHEMISTRY
A European Journal

A Journal of
ChemPubSoc Europe

Accepted Article

Title: Reaction Kinetics Direct a Rational Synthesis of an HIV-1 Inactivator of Nucleocapsid Protein 7 and Provide Mechanistic Insight into Cellular Metabolism and Antiviral Activity

Authors: Herman Nikolayevskiy, Michael T Scerba, Jeffrey R Deschamps, and Daniel H. Appella

To be cited as: *Chem. Eur. J.* 10.1002/chem.201801253

Link to VoR: http://dx.doi.org/10.1002/chem.201801253

Supported by
ACES

WILEY-VCH

10.1002/chem.201801253

WILEY-VCH

COMMUNICATION

Reaction Kinetics Direct a Rational Synthesis of an HIV-1 Inactivator of Nucleocapsid Protein 7 and Provide Mechanistic Insight into Cellular Metabolism and Antiviral Activity

Herman Nikolayevskiy,[a] Michael T. Scerba,[a] Jeffrey R. Deschamps,[b] Daniel H. Appella*[a]

Abstract: Mercaptobenzamide thioester SAMT-247 is a non-toxic, mutation-resistant HIV-1 maturation inhibitor with a unique mechanism of antiviral activity. NMR spectroscopic analyses of model reactions that mimic the cellular environment answered fundamental questions about the antiviral mechanism and inspired a high-yielding (64% overall), scalable (75 mmol), and cost-effective ($4/mmol) three-step synthesis that will enable additional preclinical evaluation.

A formidable repertoire of >30 FDA-approved HIV inhibitors[1] successfully decreased AIDS-related mortality by 43% between 2010 and 2015.[2] Despite such progress, high annual costs (>$20,000 per person),[3] long-term toxicity,[4] drug resistance,[4] and poor accessibility[2] have complicated global HIV-management efforts, particularly in the third world. In the absence of a cure, there is a continued and critical need for novel antiviral medicines that are inexpensive, nontoxic, mutation-resistant, and synthetically accessible.

HIV Nucleocapsid Protein 7 (NCp7), a 55-amino acid portion of the HIV Gag polyprotein, has attracted significant attention[5] as a next-generation target due to its highly conserved nature and its pivotal role at many points of the viral replication cycle.[6] For HIV to replicate, NCp7 must bind to viral RNA via two zinc knuckle motifs ($CX_2CX_4HX_4C$), templating the assembly of multiple Gag polyproteins at the membrane surface to direct formation of a new viral particle. After budding, HIV protease cleaves specific locations in Gag to afford free matrix, capsid, and NCp7 proteins, which reassemble into a mature, infectious particle. Interfering in these steps leads to improper HIV maturation and loss of viral infectivity.

Mercaptobenzamide thioesters (SAMTs), such as SAMT-247 (**1**; Scheme 1), are mechanistically unique molecules that inactivate NCp7 *in vitro,*[5a, 7] induce Gag aggregation *in cellulo*,[8] and inhibit proper HIV maturation *in vivo*.[9] Additionally, SAMTs display very low toxicity to cells and animals,[8-9] and appear insusceptible to viral resistance development.[8] Topical microbicide and slow-release formulations of **1** and related derivatives have shown significant promise in preventing HIV transmission in macaque models.[10] As such, **1** is an ideal candidate for further preclinical evaluation; however, the lack of an efficient synthesis (Scheme S1),[7a, 11] as well as gaps in the basic understanding of how this molecule inhibits HIV maturation without toxicity, are both hindering preclinical development.

The anti-HIV activity and high therapeutic index of SAMTs (defined as TC_{50}/EC_{50}) is particularly surprising given the range of potential reactivity for these molecules. The thioester group of **1** is known to react productively with the C-terminal zinc knuckle at Cys-36 (Scheme 1),[12] yet acetyl transfer to other available nucleophiles is also likely, including proteinogenic amino acids (S – Cys; N – Lys; O – Ser, Thr, Tyr), free cytosolic thiols (GSH), and the bulk medium (H_2O). Following acetyl transfer, the corresponding thiol **2** can be re-acetylated *in cellulo* with acetyl-CoA, such that **1** is regenerated.[8] The ability of **1** to display antiviral activity is likely a function of thioester–nucleophile exchange kinetics and their impact on the stability, availability, and chemoselectivity of the molecule.

In collaboration, we recently demonstrated that the C-terminal zinc knuckle of NCp7 is in equilibrium with a minor, unligated form, where Cys-36 loses coordination to the zinc ion.[13] The relevance of this minor species in the proposed mechanism of Gag denaturation, which involves initial acetylation of Cys-36 by **1**, followed by intramolecular acetyl transfer to Lys-38 and subsequent zinc ejection (Scheme 1),[12] will also depend on the rate of thioester–nucleophile exchange, particularly in relation to the lifetime of the minor species.

Lastly, as a consequence of zinc ejection, previously ligated NCp7 cysteines become prone to disulfide formation, leading to cross-linked Gag aggregates.[8] The propensity of aryl thiols to participate in redox chemistry suggests that if the kinetics of oxidation and acylation are comparable, **2** may play a previously undisclosed, catalytic role in the formation of inter-Gag disulfides.

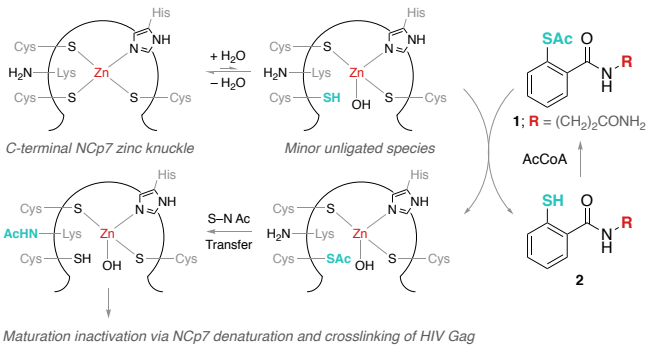

Scheme 1. Proposed mechanism of SAMT-247 (**1**)–induced HIV inactivation.

[a] Dr. H. Nikolayevskiy, Dr. M. T. Scerba, Dr. D. H. Appella*
Synthetic Bioactive Molecules Section, Laboratory of Bioorganic Chemistry (LBC)
National Institute of Diabetes and Digestive and Kidney Diseases (NIDDK), National Institutes of Health (NIH)
8 Center Drive, Room 404, Bethesda, MD 20892 (USA)
E-mail: appellad@niddk.nih.gov
[b] Dr. J. R. Deschamps
Naval Research Laboratory, Code 6910
4555 Overlook Ave. SW, Washington D.C., 20375 (USA)

Supporting information for this article is given via a link at the end of the document.

10.1002/chem.201801253

COMMUNICATION

Elegant work by Whitesides and coworkers on the kinetics of thiol–thioester exchange and thioester hydrolysis[14] inspired us to conduct a comprehensive analysis of SAMT acetylative and oxidative pathways. We present in this manuscript a deeper understanding of the basic properties and reaction kinetics of **1** toward nucleophiles under conditions designed to simulate the cellular environment. With insight into the kinetic reactivity of **1**, we propose a detailed model that informs how **1** likely exists in cells and how it reacts with HIV NCp7 and denatures Gag. Furthermore, we uniquely apply the reactivity of **1** under conditions of metabolic mimicry to design a more efficient and economical synthesis that should enable further preclinical studies.

The first step in our analysis was to experimentally measure the thiol pKa in **2**. Although a large number of fluorometric and spectroscopic techniques have been developed for the determination of pKa and kinetic parameters,[15] we selected to use NMR spectroscopy as the chemical shifts of all relevant species were found to be sufficiently resolved.[16] To quantify pKa, the thiol **2** was dissolved in a deoxygenated solution (93:7) of H_2O/D_2O, allowing for deuterium-frequency locking and shimming while avoiding significant deviation from a native aqueous environment. The pH of the resulting solution was adjusted with 0.1 M NaOH or 0.1 M HCl under a blanket of nitrogen (16–25 data points per trial in the pH range 2–11), and a water-suppressed ^{1}H NMR spectrum was attained. Tracking the chemical shift changes of H-4 (Figure 1A; 7.48 ppm – 7.80 ppm), a 4PL sigmoidal plot was constructed; the inflection point of the resulting curve (log IC_{50} output using Prism 7) was interpreted to be the pKa (Figure 1C). Repeated in triplicate, the pKa of the thiol **2** was thus determined to be 5.83 ± 0.04, suggesting the presence of a significant amount of thiolate under physiological conditions, and high aqueous solubility during synthetic manipulations.

In cells and also during purification steps, **1** could acetylate a variety of nucleophiles, such as sulfur, nitrogen, and oxygen, as well as undergo background hydrolysis. To obtain insight into how rapidly nucleophiles are acetylated by **1**, nucleophile–thioester exchange rates were determined for mimics of three intracellular nucleophiles: the thiol **3**, the amine **4**, and water at 25 °C (Figure 1B). Experiments were performed in a deoxygenated solution (93:7) of PBS 10X buffer/D_2O (pH adjusted to 7.2 ± 0.1 with 0.5 M NaOH). Tracking the loss of H-7 relative to a *tert*-butanol internal standard over the course of minutes (S–S exchange for reaction of **1**+**3**), hours (S–N exchange for reaction of **1**+**4**), or days (S–O exchange for hydrolysis), rate constants (second order for **1**+**3** and **1**+**4**, apparent pseudo-first order for hydrolysis) were obtained from appropriate integrated rate law plots, in accordance with the protocol described by Whitesides et al.[14] The rate constants thus attained differed by multiple orders of magnitude [**1**+**3**: 84 ± 11 $M^{-1}s^{-1}$; **1**+**4**: (8.8 ± 0.1) × 10^{-1} $M^{-1}s^{-1}$; hydrolysis: (9.68 ± 0.04) × 10^{-7} M^{-1}], corroborating mechanistic observations that zinc ejection from the C-terminal zinc finger of HIV-1 Gag NCp7 results from initial intermolecular acetylation of the sulfur of Cys-36 by **1**, followed by intramolecular transacetylation to Lys-38.[12] The high rate of thiol–thioester exchange (half-life ≈ 19 min; Figure 1D) suggested that the nucleophile–leaving group pairing of **2** and **3** may react rapidly in other reaction manifolds (e.g. thiol–disulfide exchange), and is consistent with recent data from Deshmukh et al., which suggests that SAMTs target a minor excited state (1.2%; lifetime > 5 ms) of the C-terminal zinc finger, in which the sulfhydryl of Cys-36 is unbound and significantly more nucleophilic.[13] Furthermore, the surprising stability of **1** in pH 7.2 buffer (half-life ≈ 8 days; Figure 1D) suggested that temporary exposure to neutral aqueous conditions would result in negligible hydrolysis.

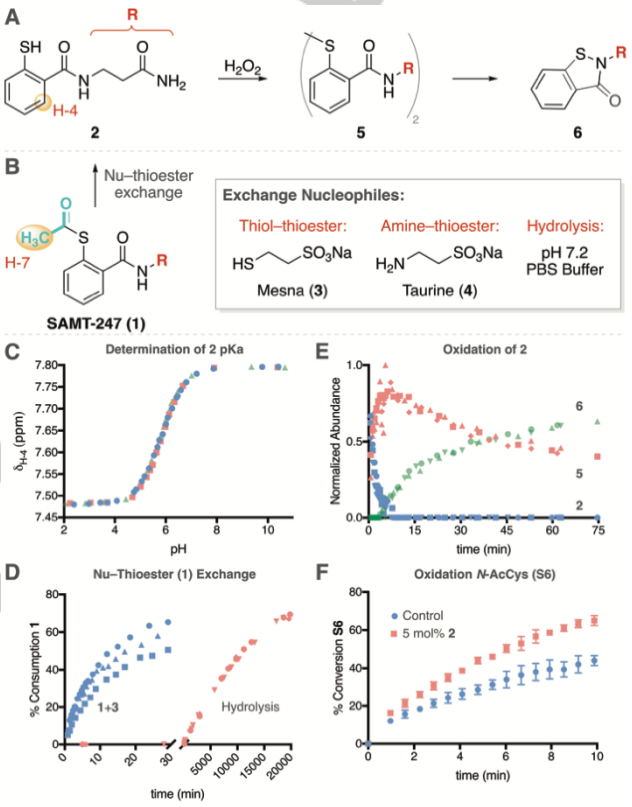

Figure 1. A) Oxidation of the thiol **2** with H_2O_2. B) Nucleophile–thioester exchange between SAMT-247 (**1**) and nucleophiles Mesna (**3**), Taurine (**4**), or pH 7.2 PBS buffer to produce the thiol **2**. C) Sigmoidal plot of H-4 (of the thiol **2**) chemical shift changes as a function of pH. D) Consumption of SAMT-247 (**1**) as a function of time for thiol–thioester (**1**+**3**) exchange and hydrolysis. Blue shapes represent triplicate data points for thiol–thioester exchange, while pink shapes represent triplicate data points for hydrolysis. E) Normalized triplicate abundance trace for the oxidation of the thiol **2** (blue) with H_2O_2 to the disulfide **5** (pink), followed disproportionation to the benzisothiazolinone **6** (green). ^{1}H NMR data normalized to largest abundance of **5** relative to *tert*-butanol internal standard. F) Oxidation rate of *N*-acetyl-L-cysteine (**S6**) to *N*,*N*'-diacetyl-L-cystine (**S7**) with 0.5 equiv H_2O_2 in the presence or absence of 5 mol% **2** (repeated in triplicate).

Lastly, we examined the susceptibility of the thiol in **2** to oxidation (which could inform how this molecule is metabolized under oxidative stress[17] in cells). The rate of **2** oxidation upon exposure to 30% hydrogen peroxide (2.3 equiv) in a solution (70:25:5) of PBS 10X buffer/DMSO-d_6/D_2O (25 °C) is displayed in Figure 1E. Qualitatively, the thiol **2** is rapidly consumed to produce the disulfide **5** (half-life ~ 1 min), followed by a more gradual disproportionation to the benzisothiazolinone **6** (half-life ~ 45 min). Due to poor aqueous solubility, **5** was observed to precipitate in solutions containing less than 25% v/v DMSO-d_6. Without sufficient amounts of DMSO, disulfide **5** precipitates before the

10.1002/chem.201801253

slower disproportionation reaction can occur to form **6**. In addition, we measured the effect of 5 mol% **2** on the rate of oxidation of an exogenous thiol [*N*-acetyl-L-cysteine (**S6**)] after exposure to 30% hydrogen peroxide (0.5 equiv) in a deoxygenated solution (93:7) of PBS 10X buffer/D_2O (pH adjusted to 7.19 ± 0.02 with 0.5 M NaOH; Figure 1F). Due to the electrophilicity of **5**, **6**, and the mixed disulfide of **2** and *N*-acetyl-L-cysteine (**S6**), we anticipated **2** would exert a catalytic influence under oxidative conditions, furnishing the disulfide *N*,*N'*-diacetyl-L-cystine (**S7**) after turnover (Scheme S4). Repeated in triplicate, **2** appears to accelerate the oxidation of *N*-acetyl-L-cysteine (**S6**) by a factor of ~1.5, suggesting that **2** is a competent catalyst for *in vitro* disulfide formation, and may contribute to Gag crosslinking *in cellulo*.

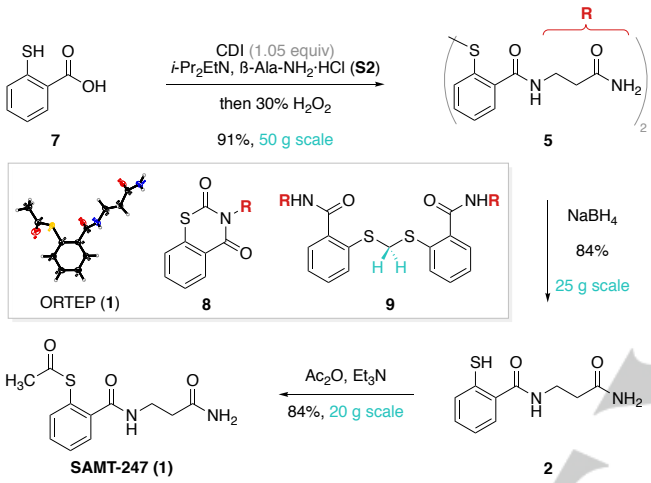

Scheme 2. Synthesis of SAMT-247 (**1**).

The kinetic parameters and molecular properties described heretofore inspired a three-step synthetic strategy (Scheme 2), carefully optimized to avoid deleterious late-stage workup or purification, whose merits include scalability (75 mmol), efficiency (64% overall yield), and cost-effectiveness ($4/mmol). Due to the poor solubility and lack of disproportionation reactivity of the disulfide **5** in water, we anticipated that initial formation of the thiol **2**, followed by oxidative workup, would provide **5** in high purity after filtration. To this end, thiosalicylic acid (**7**) was initially activated with carbonyldiimidazole (CDI; 1.05 equiv) and di-*iso*-propylethylamine, providing the acyl imidazole *in situ*, followed by amide bond formation with freshly prepared β-alanamide·HCl (**S2**; see SI for synthesis). Proper stoichiometry of CDI was important in this step as excess CDI lead to the formation of the imide **8**. Moreover, certain solvents with electrophilic functionality were found to be non-innocent in the presence of **2** and should be avoided; in particular, dichloromethane reacted with **2** to afford dithioacetal **9**. Under optimal conditions, the unpurified reaction mixture was concentrated, diluted with water, and treated with 30% H_2O_2 (2 portions, 0.20 equiv each), precipitating the disulfide **5**; as anticipated, disproportionation to **6** was not observed. The high aqueous solubility of all byproducts (imidazole: 633 g/L; di-*iso*-propylethylammonium chloride: > 4.01 g/L[18]) enabled facile isolation of **5** after several aqueous washes (91% overall yield).

After thorough drying, **5** was ground into a fine powder, suspended in a solution of methanol–tetrahydrofuran (3:1), and subjected to reduction via portion-wise addition of sodium borohydride. Due to the poor solubility of **5** under the reaction conditions, the high surface area afforded through grinding was critical for achieving full conversion. Upon concentration, the product mixture containing **2** was diluted with water and acidified to pH 1–2 with concentrated hydrochloric acid. The resulting precipitate was filtered, providing the mercaptobenzamide **2** in 84% yield. As a consequence of thiol pKa (5.83 ± 0.04), minimal washing of **2** with low temperature (< 10 °C) water was critical to avoiding excessive product loss. The thiol thus attained often contained ~5% of the disulfide **5**, resulting from re-oxidation during the workup procedure. This contamination was exacerbated at larger reaction scales. To address this issue, we relied on our experimental data from the kinetics of thiol–thioester exchange (Figure 1D) and *N*-acetyl-L-cysteine (**S6**) oxidation (Figure 1F), which suggested that the disulfide **5** may react rapidly with the thiol **3**. Indeed, addition of **3** (0.27 equiv) to the product mixture prior to acidification reduced reoxidation to **5** to < 1%.

Finally, acetylation of the mercaptobenzamide **2** with acetic anhydride and triethylamine in *N*,*N*-dimethylformamide proceeded in < 5 min to furnish SAMT-247 (**1**; 84%), the structure of which was confirmed by X-ray crystallography (Scheme 2). Notably, the triethylammonium acetate byproduct is volatile, obviating the need for aqueous workup or column chromatography. Despite extensive efforts, *N*,*N*-dimethylformamide (~1%) could not be completely removed via rotary evaporator (50 °C, < 10 torr). Instead, the concentrated product mixture was sequentially diluted with toluene, followed by a 4:1 toluene–ethanol mixture, and *N*,*N*-dimethylformamide was removed azeotropically using a rotary evaporator after each dilution. This protocol successfully replaced *N*,*N*-dimethylformamide, a class 2 solvent whose tolerated concentration in drug formulations is ~880 ppm, with ethanol (~1%), a class 3 solvent, tolerated at concentrations of ~5000 ppm.[19] We hypothesized that since **1** proved stable in pH 7.2 buffer (Figure 1D), trace ethanol could be completely removed via azeotropic distillation with water. However, **1** has relatively poor aqueous solubility (5 g/L) so the scalability of this approach was limited by the time required to remove water via a rotary evaporator. Azeotropic distillation of 6.63 mmol **1** was successful (350 mL H_2O; < 1 h required), but thioester hydrolysis was observed on larger scales.

The antiviral activity and toxicity profiles of **1** before and after azeotropic distillation with water were evaluated in CEM-SS cells.[20] SAMT-247 (**1**) of both purities was nontoxic (TC_{50} >100 μM) and inhibited virus-induced cytopathic effects at concentrations comparable to previous reports[8] (EC_{50} values of 1.3 ± 0.7 μM and 0.9 ± 0.3 μM, respectively). Based on these data, we propose that **1** containing residual ethanol is sufficiently pure for further preclinical evaluation.

Our synthetic observations, in combination with our examination of reaction kinetics and pKa, provide new insights into the behavior of **1** in cells (Scheme 3). On the basis of nucleophile–thioester exchange kinetics, the lifetime of **1** in the cellular milieu is likely low. Productive reactivity with the minor unligated thiol of Cys-36 within the C-terminal zinc knuckle of NCp7,[13] or unproductive reactivity with high abundance

cytoplasmic thiols (such as CoA or glutathione) would rapidly convert **1** to the major species **2**, which predominantly exists as the thiolate in cells under physiological conditions (pH 7.4). While non-enzymatic hydrolysis is likely negligible, the slower direct acyl-transfer to proteinogenic amines may be a viable, albeit minor, pathway. Although **1** may be regenerated from **2** via acetyl-CoA,[8] the formation of **1** is strongly disfavored at equilibrium, as demonstrated by the reaction of **1** with **3**.

Table 1. Antiviral activity [EC_{50} (μM)], toxicity [TC_{50} (μM)], and therapeutic index (TI) of SAMT-247 (**1**).

Compound	EC_{50} (μM)	TC_{50} (μM)	TC_{50}/EC_{50} (TI)
1 + 1% EtOH	1.3 ± 0.7	>100	>77
1	0.9 ± 0.3	>100	>100

Alternatively, in the presence of H_2O_2, O_2, or other reactive oxygen species (ROS) in cells, **2** may be oxidized to a mixed disulfide (**10**). From our experience in synthesizing **6**, we propose that direct oxidation from **2** to the benzisothiazolinone **6** is unlikely. Although **10** may disproportionate to **6** *in vitro*, the high reactivity of both **6** and **10** towards thiol nucleophiles, as demonstrated by the mercaptobenzamide–catalyzed oxidation of *N*-acetyl-L-cysteine (**S6**), suggests that the equilibrium concentration of **10**, and particularly **6**, is also low.

Nevertheless, fast acetylative and oxidative reaction kinetics, in combination with the capacity of **1**, **6**, and **10** to regenerate from the thiolate **2**, suggest that loss of HIV infectivity via **1**–mediated NCp7 denaturation, followed by **6**– or **10**–catalyzed Gag crosslinking, is a viable mechanism of action for this class of antivirals. Moreover, low equilibrium concentrations of active metabolites (**1**, **6**, and **10**) may explain the low toxicity and micromolar activity of the SAMTs.

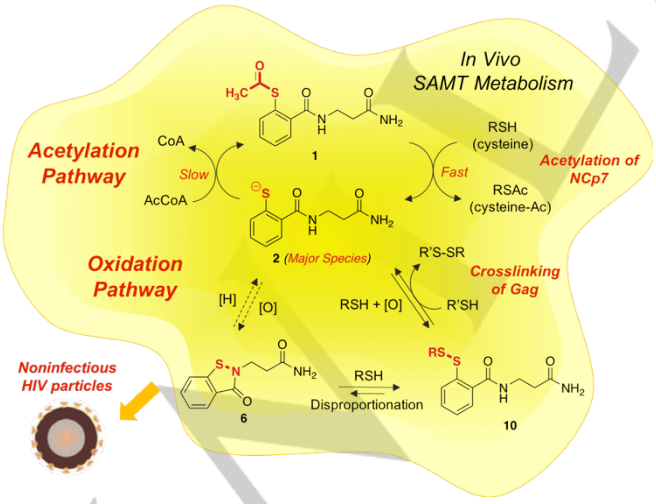

Scheme 3. Proposed acetylative and oxidative mechanistic cycles for *in vivo* SAMT-247 (**1**)–induced HIV inactivation via NCp7 denaturation and formation of Gag crosslinks.

In summary, a detailed investigation of SAMT kinetics and molecular properties has provided insight into both productive and unproductive SAMT reaction pathways in cells. The predominance of thiol–thioester exchange (as compared to other nucelophiles), the high equilibrium abundance of the thiolate **2** (as compared to the more reactive metabolites **1**, **6**, and **10**), and the application of interconnected acetylative and oxidative reaction manifolds to the mechanism of HIV inactivation, are particularly notable. Moreover, it led to a three-step synthesis of SAMT-247 (**1**), which was conducted on 75 mmol scale with 64% overall yield, utilizes inexpensive reagents ($4/mmol), and avoids any chromatography.

Acknowledgements

This research was supported by the Intramural Research Program of NIDDK, NIH. We thank Tracy L. Hartman and Robert W. Buckheit, Jr. of ImQuest Biosciences (Frederick, MD) for performing antiviral assays, John Lloyd for performing mass spectrometry, and Robert O'Connor for assistance with NMR. The X-ray crystallographic work was supported by NIDA through Interagency Agreement (IAA) ADA17001 with the Naval Research Laboratory (NRL).

Keywords: HIV • nucleocapsid • mercaptobenzamide • scalable synthesis • antiviral mechanism • reaction kinetics

[1] A list of currently approved inhibitors can be found on the U.S. Food and Drug Administration website, titled: Antiretroviral drugs used in the treatment of HIV infection. https://www.fda.gov/forpatients/illness/hivaids/treatment/ucm118915.htm. Page last updated: 8/9/16.

[2] Estimate from "Global AIDS Update 2016," prepared by Joint United Nations Programme on HIV/AIDS. Available at: http://www.unaids.org/sites/default/files/media_asset/global-AIDS-update-2016_en.pdf. Last accessed: 11/28/17.

[3] K. A. Gebo, J. A. Fleishman, R. Conviser, J. Hellinger, F. J. Hellinger, J. S. Josephs, P. Keiser, P. Gaist, R. D. Moore, *AIDS (London, England)* **2010,** *24*, 2705-2715.

[4] D. A. Solomon, P. E. Sax, *Curr. Opin. HIV AIDS* **2015,** *10*, 219-225.

[5] a) L. Sancineto, N. Iraci, O. Tabarrini, C. Santi, *Drug Discovery Today* **2017**; b) D. Garg, B. E. Torbett, *Virus Res.* **2014,** *193*, 135-143; c) H. de Rocquigny, V. Shvadchak, S. Avilov, C. Z. Dong, U. Dietrich, J. L. Darlix, Y. Mely, *Mini Rev. Med. Chem.* **2008,** *8*, 24-35; d) V. Goldschmidt, L. M. Miller Jenkins, H. de Rocquigny, J.-L. Darlix, Y. Mély, *HIV Ther.* **2010,** *4*, 179-198.

[6] a) J. L. Darlix, J. L. Garrido, N. Morellet, Y. Mély, H. d. Rocquigny, Properties, Functions, and Drug Targeting of the Multifunctional Nucleocapsid Protein of the Human Immunodeficiency Virus. In *Adv. Pharmacol.*, Academic Press2007; Vol. 55, pp 299-346; b) J. A. Thomas, R. J. Gorelick, *Virus Res.* **2008,** *134*, 39-63.

[7] a) L. M. Miller Jenkins, J. C. Byrd, T. Hara, P. Srivastava, S. J. Mazur, S. J. Stahl, J. K. Inman, E. Appella, J. G. Omichinski, P. Legault, *J. Med. Chem.* **2005,** *48*, 2847-2858; b) P. Srivastava, M. Schito, R. J. Fattah, T. Hara, T. Hartman, R. W. Buckheit, J. A. Turpin, J. K. Inman, E. Appella, *Biorg. Med. Chem.* **2004,** *12*, 6437-6450.

[8] L. M. M. Jenkins, D. E. Ott, R. Hayashi, L. V. Coren, D. Wang, Q. Xu, M. L. Schito, J. K. Inman, D. H. Appella, E. Appella, *Nat. Chem. Biol.* **2010,** *6*, 887-889.

[9] a) M. L. Schito, A. Goel, Y. Song, J. K. Inman, R. J. Fattah, W. G. Rice, J. A. Turpin, A. Sher, E. Appella, *AIDS Res. Hum. Retroviruses* **2003,** *19*, 91-101; b) M. L. Schito, A. C. Soloff, D. Slovitz, A. Trichel, J. K. Inman, E. Appella, J. A. Turpin, S. M. Barratt-Boyes, *Curr. HIV Res.* **2006,** *4*, 379-386.

[10] a) G. S. Wallace, C. Cheng-Mayer, M. L. Schito, P. Fletcher, L. M. Miller Jenkins, R. Hayashi, A. R. Neurath, E. Appella, R. J. Shattock, *J. Virol.* **2009,** *83*, 9175-9182; b) S. R. Ugaonkar, J. T. Clark, L. B. English, T. J. Johnson, K. W. Buckheit, R. J. Bahde, D. H. Appella, R. W. Buckheit, P. F. Kiser, *J. Pharm. Sci.* **2015,** *104*, 3426-3439; c) Y. Yang, J. Zhu, M.

Hassink, L. M. M. Jenkins, Y. Wan, D. H. Appella, J. Xu, E. Appella, X. Zhang, *Emerging Microbes Infect.* **2017,** *6*, e40.

[11] R. J. Bahde, D. H. Appella, W. C. Trenkle, *Tetrahedron Lett.* **2011,** *52*, 4103-4105.

[12] L. M. M. Jenkins, T. Hara, S. R. Durell, R. Hayashi, J. K. Inman, J.-P. Piquemal, N. Gresh, E. Appella, *J. Am. Chem. Soc.* **2007,** *129*, 11067-11078.

[13] L. Deshmukh, V. Tugarinov, D. H. Appella, G. M. Clore, *Angew. Chem. Int. Ed.* **2018**, *57*, *Just Accepted*.

[14] P. J. Bracher, P. W. Snyder, B. R. Bohall, G. M. Whitesides, *Origins Life Evol. Biospheres* **2011,** *41*, 399-412.

[15] J. Reijenga, A. v. Hoof, A. v. Loon, B. Teunissen, *Anal. Chem. Insights* **2013,** *8*, ACI.S12304.

[16] A. D. Gift, S. M. Stewart, P. Kwete Bokashanga, *J. Chem. Educ.* **2012,** *89*, 1458-1460.

[17] M. Masiá, S. Padilla, M. Fernández, C. Rodríguez, A. Moreno, J. A. Oteo, A. Antela, S. Moreno, J. del Amo, F. Gutiérrez, B. CoRis, *PLoS One* **2016,** *11*, e0153456.

[18] The aqueous solubility of di-iso-propylethylamine, triethylamine, and triethylammonium chloride are reported to be 4.01 g/L, 112 g/L, and 1440 g/L, respectively. Although solubility data for di-iso-propylethylammonium chloride could not be found, it is likely to be significantly higher than 4.01 g/L.

[19] USP <467> Residual Solvent Compliance Requirements. Accessed on 8/25/17 from: https://hmc.usp.org/sites/default/files/documents/HMC/GCs-Pdfs/c467.pdf

[20] P. L. Nara, P. J. Fischinger, *Nature* **1988,** *332*, 469.

10.1002/chem.201801253

WILEY-VCH

Entry for the Table of Contents (Please choose one layout)

Layout 1:

COMMUNICATION

NMR spectroscopic analyses of model reactions that mimic the cellular environment answered fundamental questions about the antiviral mechanism of HIV inactivator SAMT-247 and inspired a high-yielding (64% overall), scalable (75 mmol), and cost-effective ($4/mmol) three-step synthesis that will enable additional preclinical evaluation.

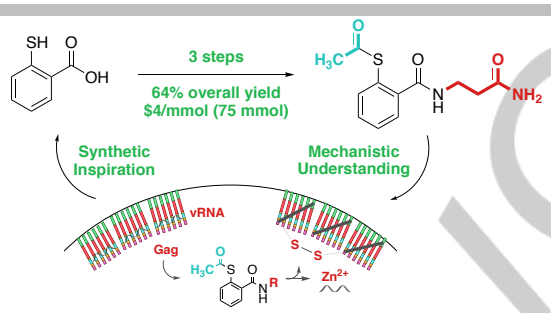

Dr. Herman Nikolayevskiy, Dr. Michael T. Scerba, Dr. Jeffrey R. Deschamps, Dr. Daniel H. Appella[a]*

Page No. – Page No.

Reaction Kinetics Direct a Rational Synthesis of an HIV-1 Inactivator of Nucleocapsid Protein 7 and Provide Mechanistic Insight into Cellular Metabolism and Antiviral Activity